FIBRES & TEXTILES in Eastern Europe

sciendo

FIBRES & TEXTILES in Eastern Europe

Research Article • DOI: 10.2478/ftee-2023-0034 FTEE • 31(4) • 2023 • 38–45

# Mechanical Properties of Textile-Reinforced Composites with a 3D Printed Core

Jakub Szary[1]*, Marcin Barburski*[1], Jacek Świniarski[2]

[1] *Institute of Architecture of Textiles, Faculty of Material Technologies and Textile Design, Lodz University of Technology, Zeromskiego 116, 90-543 Lodz, Poland*
[2] *Department of Strength of Materials, Faculty of Mechanical Engineering, Lodz University of Technology, Stefanowskiego 1/15, 90-924 Lodz, Poland*
** Corresponding author. E-mail: jakub.szary@dokt.p.lodz.pl; marcin.barburski@p.lodz.pl*

**Abstract**
The article discusses the mechanical properties of glass fiber epoxy composites with three types of textile structures. Braided, knitted and woven sleeves were placed on a 3D printed flat core and impregnated with resin using the vacuum bag method. The 3-point flexural and tensile tests were performed. The results were compared with those of 3D-printed flat bars and proved that woven textile structures increase the strength and modulus of elasticity, whereas braided and knitted structures only increase the moduli. The advantages, drawbacks and failure modes of each reinforcement structure are also discussed including the drapeability on the spatial core.

**Keywords**
additive manufacturing, mechanical properties, composite, 3D printed core, textile reinforcement.

## 1. Introduction

3D printing (3DP) technology is present in most fields of engineering and technical sciences, including materials engineering and medical and life sciences, especially in the production processes of individually designed products. This technology provides additional possibilities, particularly for the production of fast and custom-made end-use parts [1].

The additive manufacturing (AM) market was valued at USD 14.39 billion in 2021, with a projection in 2030 to reach USD 83.56 billion at a CAGR of 21.2% during the forecast period [2]. The most important field of R&D is material engineering, in which researchers attempt to improve and develop new materials. Moreover, research has been focused on reducing high production costs, extending applications to large structures and mass production, as well as on improving the mechanical properties [1].

Polymers are usually used in the aerospace, automotive, sports, medical, architectural, and toy industries and are most commonly used in additive technologies. Due to their high production costs, metals are used in the aerospace, defence, and automotive industries to manufacture complex shaped parts. Ceramics are typically used in biomaterials, tissue engineering, and as an ingredient of concrete in the construction industry. Each type of material can be processed using different AM technologies, classified into seven categories: powder bed fusion, material extrusion, material jetting, vat photopolymerization, binder jetting, directed energy deposition, and sheet lamination [3]. They all have advantages and disadvantages and are used depending on the application requirements.

In this study, the powder bed fusion (PBF) technology was used based on the selective sintering of powder material in the bed using thermal energy. This allows for the manufacturing of high-precision parts with complex structures. The main advantage of this method is that the support is a non-sintered powder that is easy to remove, unlike other AM technologies where the support must be removed manually or chemically [4–6]. Usually, additional post-processing is sandblasting, which does not require post-curing, as in binder jetting or vat photopolymerization [6,7]. A drawback of PBF is that it is a slow process that incurs high cost. However, it can be optimized by printing many elements in a single process [1]. In addition, PBF has a limited number of materials compared to the most common and well-known technology: material extrusion (ME). However, the use of engineering plastic materials, such as polyamide, with good mechanical properties allows the replacement of parts manufactured by injection molding. ME also allows for the use of high-strength fiber reinforcement composites, but the filament can be placed only layer-by-layer, which causes low interlayer adhesion and low mechanical strength in one orientation [4]. Moreover, parts typically have low fiber volume fractions (35%) and high void contents (12%), which result in poor mechanical properties [8,9]. Additional support must be provided during the printing process. Many materials used in other technologies have low heat deflection temperatures or brittle parts, which limits their application [5,6].

The limitations of AM in the form of anisotropy of printed elements and the high cost of using metal materials are the main reasons to develop composites with a 3D printed polymeric core and an outer layer in the form of fiber reinforcement. This study examined the influence of various textile structures on the mechanical properties of manufactured composites. The main 2-D textile-forming techniques for composite reinforcement

are woven, braided, and knitted fabric, as well as technical embroidery [10,11]. The first three types allow to manufacture textile sleeves. In this study these structures were placed on a 3DP flat core and impregnated with epoxy resin using the vacuum bag method. Owing to the use of 3D printing technology and the ability to print complex shapes, the core can be used as a frame for the structure in combination with non-rigid molds, such as vacuum bags or infusion techniques. These methods can provide the opportunity to achieve high-strength custom-made parts.

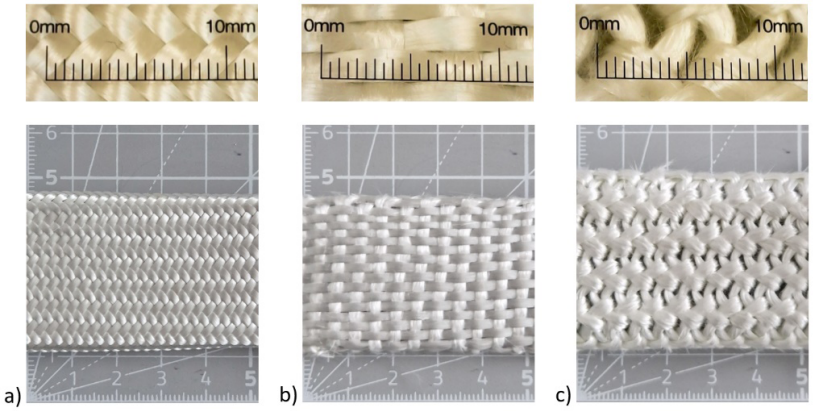


*Fig. 1. Textile reinforcement on 3DP core: a) braid, b) woven fabric, c) knitted fabric*

## 2. Materials

Three types of composites were fabricated using different textile structures: braided, woven, and knitted fabric. The rectangular core was fabricated using 3D printing (3DP) technology - powder bed fusion (PBF). The matrix was an epoxy resin, and the fiber reinforcements, in the form of sleeves, were made of E-glass yarn. Figure 1 shows the textile structures without impregnation.

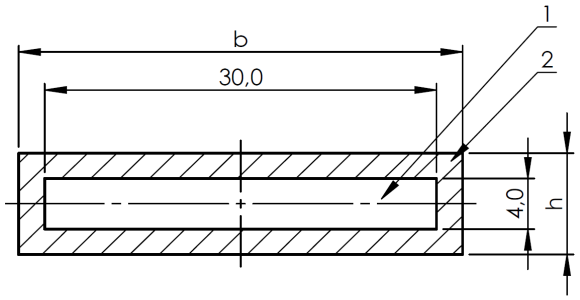


*Fig. 2. Structure of composite: 1) 3D printed core, 2) impregnated textile reinforcement*

The reinforcements were placed on rectangular 3D-printed cores and impregnated with epoxy resin using the vacuum-bag method. HAVEL Composite LH145 epoxy resin and HAVEL Composite H135 hardener were used in a ratio of 100:35 by weight. The impregnated tubular reinforcement was cured at 25 °C for at least 24 h and then machined using a milling machine. Figure 2 shows a cross section of the composites prepared.

The dimensions of the composites are presented in Table 1. The dimensions of the 3DP core remain unchanged. The difference between the outer dimensions depended on the textile structure.

The core was fabricated using 3D printing technology - powder bed fusion - on an HP Jet Fusion 3D 4200 printer called MJF-Multi Jet Fusion. PA12 powder was used with a refresh ratio of 80/20 (old/new). The layer height was set at 0.08 mm. The printing speed was 4 115 cm$^3$/h on balanced mode with solid infill, and the process finished after 15 h 22 min. The packing density was 8,98 % and the space between parts – 5 mm. The cores were positioned in the X orientation, as shown in Figure 3. The mechanical properties depend on the orientation of the sample during 3D printing, and research has shown that the Z-orientation has 40 % greater bending strength than the X-orientation [12]. The basic mechanical properties of 3DP cores are listed in Table 2.

| Textile structure | h [mm] | b [mm] |
|---|---|---|
| Braid | 5,5 | 32,5 |
| Woven fabric | 5,8 | 32,8 |
| Knitted fabric | 9,5 | 35,5 |

*Table 1. Dimensions of composites*

| Properties | Value | Unit |
|---|---|---|
| Density | 1,01 | [g/cm$^3$] |
| Tensile modulus $E_t$ (X) | 1242 ± 28 | [MPa] |
| Tensile strength $\sigma_{max}$ (X) | 47 ± 0,9 | [MPa] |
| Flexural stress $\sigma_f$ (X) | 50 ± 0,9 | [MPa] |
| Flexural modulus $E_f$ (X) | 1146 ± 51 | [MPa] |
| Elongation at break $\varepsilon_b$ (X) | 19 ± 2,8 | [%] |

*Table 2. Properties of 3D printed core*

All textile reinforcements were supplied by the Dortech EU company. The composite and textile materials parameters are presented in Table 3. E-glass yarn EC9 34 T63 from Verotex Saint-Gobain was used to make yarns by twisting in the case of braided and woven fabric and for knitted fabric by texturizing. The biaxial braid angle measured on the core was 45 ° and the picks count was 44 [1/dm]. The woven fabric weft count was 24 [1/dm] and the warp 55 [1/dm]. The knitted fabric yarn was interlaced with a density of 18 wales [1/dm] and 16 courses [1/dm]. The average density of the composites was calculated as the sample weight (core and reinforcement) per unit volume. The areal weight of each textile layer was measured. The mass fraction was calculated by dividing the

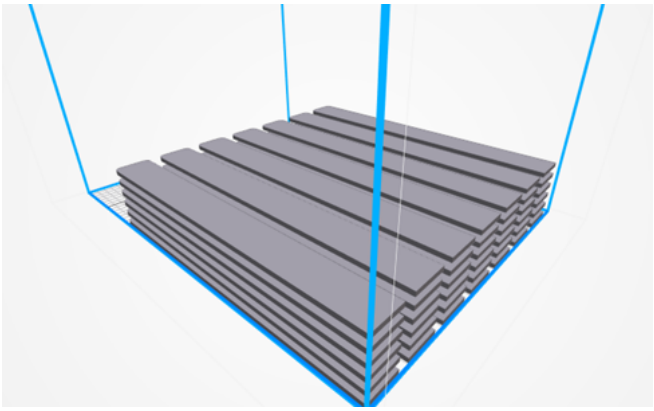

*Fig. 3. X-orientation of 3D printed core*

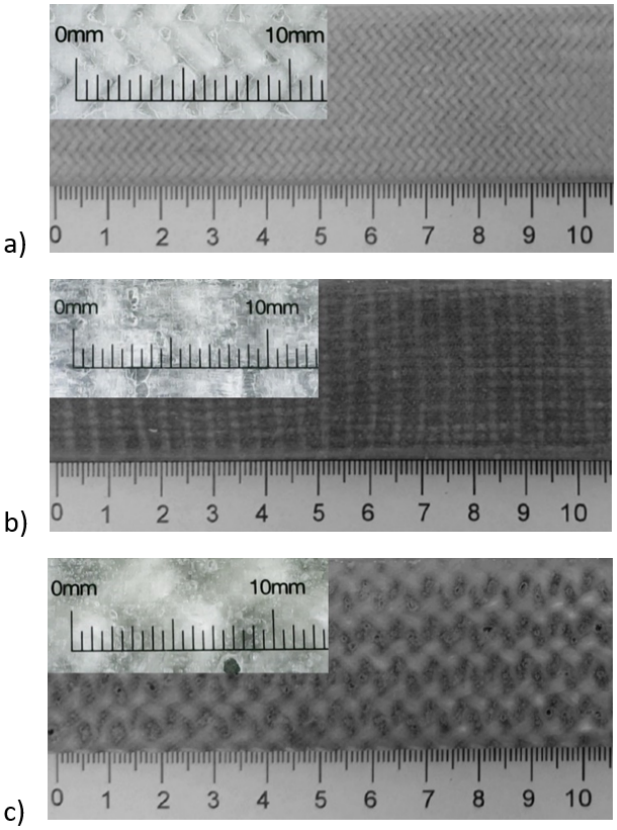


*Fig. 4. Composite reinforcement: a) braid fabric, b) woven fabric, c) knitted fabric*

| Parameter | Braid | Woven fabric | Knitted fabric |
|---|---|---|---|
| Density of composite [g/cm$^3$] | 1,17 | 1,11 | 1,23 |
| Areal weight of textile structure [g/m$^2$] | 1 100 | 800 | 4 200 |
| Areal weight of composite outer layer [g/m$^2$] | 2 340 | 1 545 | 9 310 |
| Mass fraction of composite outer layer [%] | 45,5 | 50,5 | 45 |
| Linear density of the yarn [tex] | 800 | 1200 x 800 [1] | 2 600 |
| Structure configuration | 2/2 twill | 1/1 plain | S1 [2] |

[1] *warp x weft*
[2] *manufacturer's number*

*Table 3. Parameters of composites and textile materials*

areal weight of the composite outer layer by that of the textile structure.

Figure 4 shows the composites prepared on two scales. On each one, we can find voids that result from both the method used and the textile structure.

## 3. Methods

### 3.1. Flexural test

The flexural test was performed according to ISO 14125 [13] using a 3-point bending test fixture with a registered load on a Zwick/Roell Z005. Five samples from each textile structure were tested. The test was stopped when the sample was destroyed or when the specimen made direct contact with the instrumentation surface. Based on the assumption that the unchanged cross-section of the 3D printed core in order is essential for the data to be comparable, the support spacing was set as 16 times the sample thickness: 88 mm for braided fabric, 92.8 mm for woven fabric and 152 mm for knitted fabric. The test speed was set to 1 mm/min. The diameters of the loading and support members were 5 mm. The samples were conditioned for 24 h at a temperature of 23 °C and humidity of 50 % before testing.

### 3.2. Tensile test

Tensile tests were performed according to the ISO 527-4 standard [14]. The calculation methods were based on ISO 527-1 [15]. Experiments were performed using an INSTRON universal testing machine (Model 8032). The test speed was set to 1 mm/min. To measure elongation, a 50 mm gauge length extensometer was used, in which no grips were used – Type 2; and the specimen length -was 250 mm, and the initial distance between grips – 150 mm. Five samples from each textile structure were tested.

### 3.3. Drapeability

Each textile structure was placed on a spatial element, shaped similarly as used

in knee orthopaedic braces, in order to observe its formability The cross section of the core was the same as that used for preparing the composite. Organoleptic evaluation and visual inspection were performed to determine the feasibility of using textile structures on complex and spatial cores.

## 4. Results and discussions

### 4.1. Flexural test

Five samples of each composite were tested. Bending forces were applied to the mid-span of the sample until the strain reached approximately 5 %. Figure 5 shows the flexural stress-strain curves of each composite and 3D printed core.

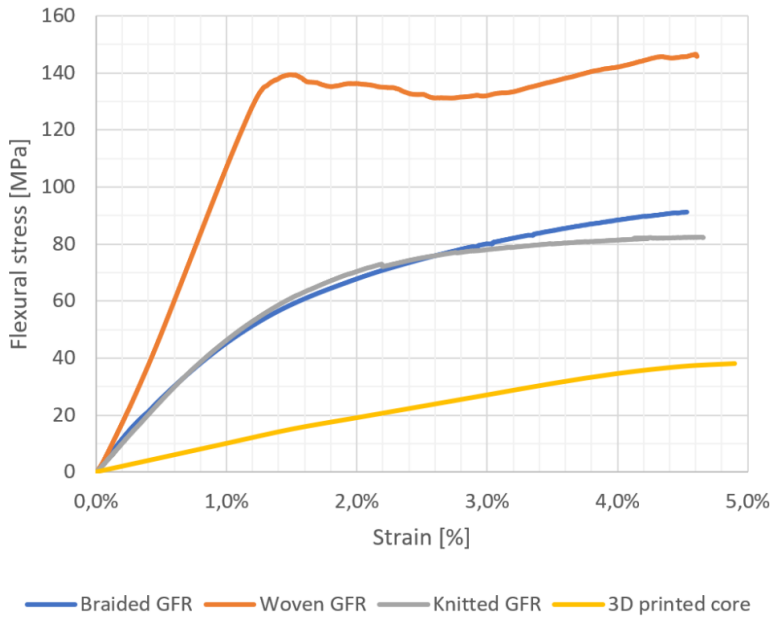


*Fig. 5. Flexural stress-strain curves of tubular glass fiber reinforcement (GFR) composites and 3D printed core*

The initial slope of the stress-strain curve was defined as the flexural modulus. The first range can be characterized as a quasi-elastic region for each textile structure. The flexural modulus was similar for the braided and knitted reinforcements and the differences were statistically insignificant, whereas the woven fabric demonstrated an approximately twice higher value. Each of the composites exhibited a higher strength than the tested 3D printed core. However, the 3DP cores did not break during testing and strains up to 5 % were within the yield point.

The flexural stress-strain curves of braided and knitted reinforcements have a similar course but can be observed to have different behaviors in the flexural strength region defined as acceptable failure modes. In the braided reinforcement curve a small drop can be observed, corresponding to the delamination of the outer layer. Transverse shear stress occured between the two different materials, such as the 3DP core and the glass/epoxy layer. Since the 3DP core did not break, the process was propagating and acting on the layer's interface. Despite the appearance of delamination between the outer facings and the core, none of the layers was damaged. Therefore, the stiffness of the structure decreased but did not completely lose its ability to carry the load. In the knitted reinforcement, the first step in the curve corresponds to the cracking of the matrix. A strain that is quasi-proportional to the acting stress only occurs in the woven structure. Two regions can be observed with a linear behavior. For the first region between a strain of 0 % and approximately 0.3 %, the slope of the curve is smaller than that in the second range and is classified as the flexural modulus. After a 0.3 % strain a higher Young's modulus occurred, which corresponded to the tensioning of the fiber in the matrix [16]. Averages of the measurements from all samples are presented in Table 4. It must be underlined that the parameters present the material as a homogeneous structure and are used to compare the materials examined. In addition, the difference in the thickness and structure of the outer layer in each textile structures may affect its composite properties as a whole multilayer structure. In fact, the effective stress depends not only on material properties but also on the sequence of layers and shear stress [17]. Therefore the mechanical properties presented (described by the effective stress) are only applicable to the structures developed and are considered potentially applicable in textile reinforcement provided that the 3DP core is the same in each composite.

The different values of the coefficient of variation may have been caused by differences in the manner in which the sleeve was applied to the 3D-printed core. The tubular shape of the textile reinforcement and the structures exhibited stretchability. The bottom layer was tensioned during the bending process, which increased the angle between yarns. To increase the repeatability, the braided or knitted sleeve should be additionally strained, which can cause difficulties without special tooling in the process of manufacturing. The flexural strength of the woven reinforcement was approximately twice that of the other reinforcements tested, indicating that the warp placed along the core transferred the highest amount of the load applied.

In Figure 6, samples after the flexural test are presented, where the brighter region is the location where the member load was applied. Each composite exhibited a different failure model; however, the outermost layer was not damaged in any of the samples.

In the braided reinforcement, the brighter region in the rectangular area indicates a delaminated ply of the composite. No fibers were damaged; the outer layer moved with the textile structure and the

| Parameter | Braid | Woven fabric | Knitted fabric |
|---|---|---|---|
| Flexural stress $\sigma_{fM}$ [MPa] | 79 ±3,5 | 140 ±5 | 73 ±4 |
| Flexural strain $\varepsilon_{fM}$ [%] | 2,9 ±0,3 | 1,3 ±0,1 | 2,2 ± 0,4 |
| Flexural modulus $E_f$ [MPa] | 5 820 ±675 | 9 330 ±575 | 5 210 ± 180 |

*Table 4. Flexural properties of glass fiber reinforcement composite*

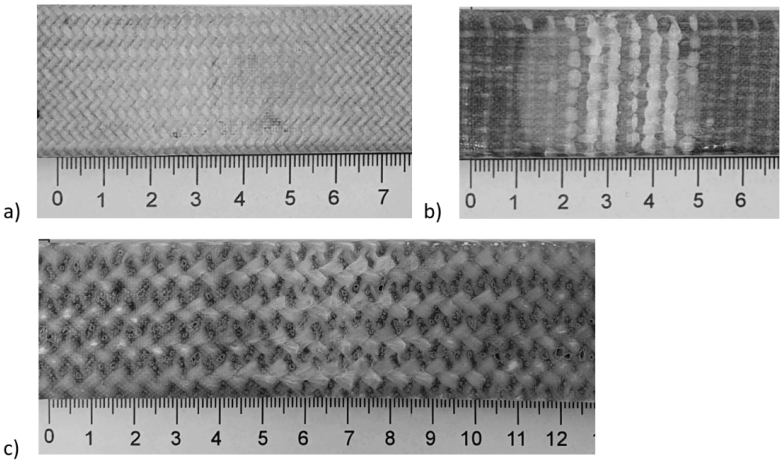


*Fig. 6. Sample after flexural test: a) braided GFR, b) woven fabric GFR, c) knitted fabric GFR*

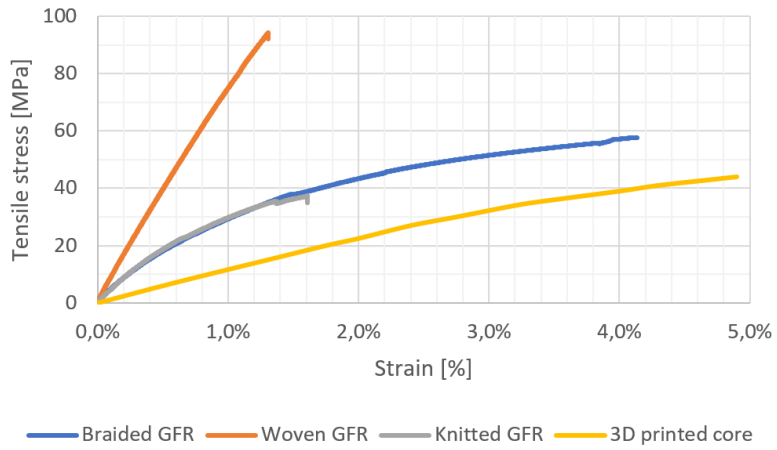


*Fig. 7. Tensile stress-strain curves of tubular glass fiber reinforcement (GFR) composites and 3D printed core*

interyarn matrix cracked. A slight change in the angle of the yarn position was observed, indicating stretching during the bending test. After the load was removed, the samples did not return to their original shape. Cracks were not observed in the cores. The failure mode was classified as interlaminar shear fracture.

The failure of the other forms of reinforcement, woven and knitted, was classified, according to the standard, as a compressive fracture [13]. The form of sample failure indicates that the matrix cracked and the fibers ruptured. Furthermore, interlaminar shear occured between the woven outer layer and the core.

## 4.2. Tensile test

Tensile tests were performed on each composite type. The test was continued until the sample broke or the samples reached 5 % of strain. Five samples of each composite were tested. Figure 7 shows the average stress-strain curves of the composites. Table 5 presents the average results and coefficients of variation for each composite.

It can be observed that the composites with braided and knitted reinforcements have a similar course, and the differences in the tensile modulus are not statistically significant, unlike in the woven fabric. The non-elastic range during the test was recorded for the braided reinforcement, and the strain was out of proportion to the stress. At a tensile strain of approximately 1.5 %, a crack in the core occurred following the rupture of the fiber. The braided reinforcements tend to be tensile in nature [18]. At the beginning of the test, the interyarn matrix cracked simultaneously and the angle between the yarns increased until the core and reinforcement broke.

The woven glass reinforcement strain-stress curve exhibited quasi-elastic behavior and a slight non proportional dependence [19]. The composite can be classified as a brittle material without a determinable yield point. Breakage occurred when the stress exceeded the elastic limit stress and tensile strain, which was also the strain at break. The Young's moduli of the samples were similar. The failure mode, such as the cracking of the matrix, begins first. Subsequently, the warp tensioning and delamination processes were observed simultaneously. The core broke next, which can be observed as a drop in the curve.

Similar to a braided structure, a nonlinear range characterizes knitted fabric reinforcement. First, at a strain of approx. 0.7 %, the textile reinforcement started to extend and break the matrix. In the second region visible damage to the matrix was observed until the core and textile structures broke. The first drop in the curve was observed and classified as the tensile strength, after which a higher strength was observed; but the outer layer of the composite cracked.

The tensile strength of the composites was lower than their bending strength. Research has shown that the bending strength-to-tensile strength ratio can

| Parameter | Braid | Woven fabric | Knitted fabric |
|---|---|---|---|
| Tensile strength $\sigma_m$ [MPa] | 37,8 ±0,4 | 94 ±16 | 23 ±1 |
| Tensile strain $\varepsilon_m$ [%] | 1,5 ±0,1 | 1,3 ±0,2 | 0,7 ± 0,1 |
| Tensile modulus $E_t$ [MPa] | 3 875 ±240 | 7 970 ±440 | 4 140 ± 130 |

*Table 5. Tensile properties of glass fiber reinforcement composite*

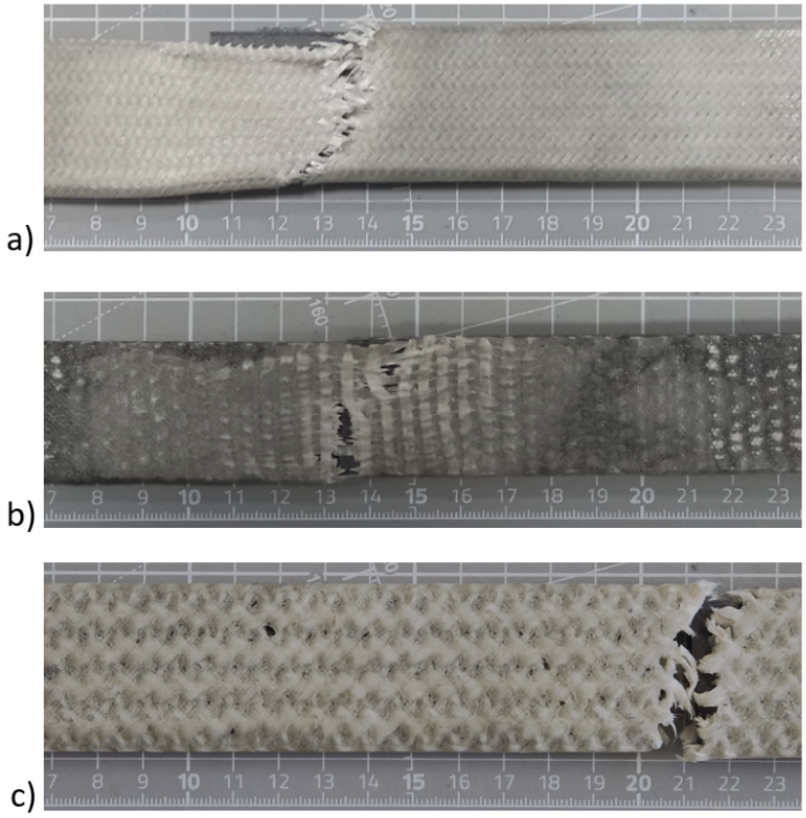


*Fig. 8. Sample after tensile test: a) braided GFR, b) woven fabric GFR, c) knitted fabric GFR*

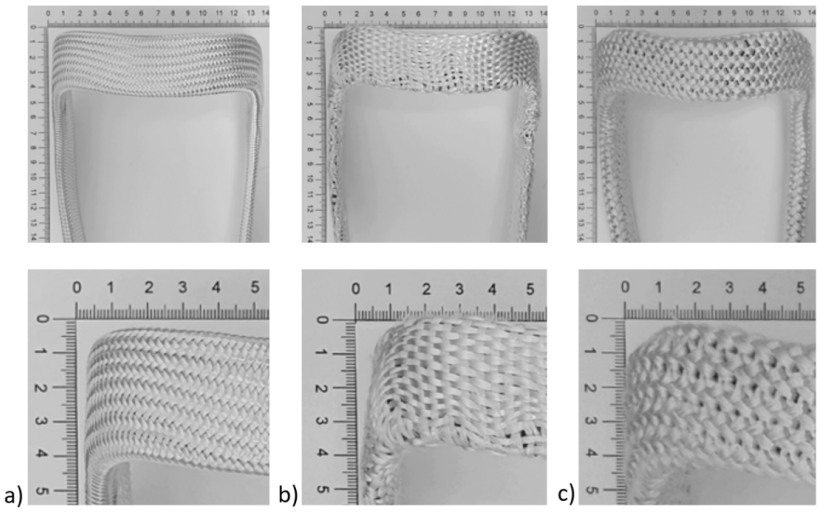


*Fig. 9. Drapeability of textile structure: a) braided , b) woven, c) knitted fabric*

reach 1.40 [20]. This dependence can be observed in the case of woven reinforcement, unlike in the other two types, where the ratio exceeds two for the braided fabric and three for the knitted fabric. These differences may indicate that the failure of the composite during the bending test occurred earlier than visible damage. It can be assumed that delamination of the textile reinforcement from the 3D-printed core occurred.

The samples obtained after the tensile tests are shown in Figure 8. Delamination occurred in the brighter regions. The reinforcement broke under different strain values. Delamination also occurred after the core cracking. The samples with a higher strain at break exhibited higher transverse strain and a structure close to the failure area in the braided tube.

## 4.3. Drapeability

The formability of each textile structure is shown in Figure 9. The spatial element shows a frame with two parallel arms that are similar in shape to the orthopaedic knee brace. The cross section of the core was the same as that used in the composite.

The best drapeability of the spatial core was shown by the braided and knitted structures. The plain weave was much worse than those of the other textile structures. It can be observed that wrinkling could negatively affect the mechanical properties. Other weaves, such as twill or satin, have better formability, but they do not resolve the compression of the fiber on the complex geometry. Research shows that woven fabric has good drapeability in the double dome form [21], but the use of a sheet of fabric that is not suitable for the application presented causes difficulties in the manufacturing process and a waste of material. However, as presented in this study, textile reinforcement with fibers placed along the acting force significantly increased the strength and modulus of the composite compared with braided and knitted fabrics. Such a structure can be

used to increase the stiffness and, due to its good formability, as a finishing layer in the infusion or vacuum bag method.

## 5. Conclusion

Additive manufacturing (AM) is a rapidly growing technology in many engineering and technical fields. The use of AM provides additional possibilities that cannot be achieved or cause difficulties in production by other technologies, such as machining, injection molding or forming processes, especially in individual piece production. This study discusses an attempt to reinforce such 3DP parts using E-glass reinforcement. The textile structures presented, such as braided, woven, and knitted fabrics in the form of sleeves. were found to be able to increase the flexural and tensile modulus. However, a higher modulus significantly decreased the elongation at break of all samples. Compared to the 3D printed part, the flexural strength increased in all cases, but the tensile strength was lowered in braided and knitted structures. In both cases, this was due to the lack of longitudinal load-bearing fibers. The tensile forces acting on the outer layer caused matrix breakage and were classified as non-acceptable failures. Delamination was also observed in the samples tested. Therefore, the attraction between the two dissimilar phases may also affect mechanical properties and should be considered in future works. The phenomenon of increasing the strength occurred in the woven structure. However, its formability in spatial geometry is very poor and wrinkling of the fibers can be observed during drapeability.

The conclusions from the experiments indicate further development of textile reinforcements in the use of high-strength composites with a 3DP core, especially with the fiber placed along the acting forces. Research shows that technical embroidery, as an outer layer of a composite, can also fulfil the requirements of such applications [11,22]. On the basis of this study, it was decided to undertake further works on the reinforcement with the UD textile structure.

## Conflict of Interest Declaration

The authors declare that they have no affiliations with or involvement in any organization or entity with any financial interests in the subject matter or materials discussed in this manuscript.

## Funding Statement

The funders had no role in the study design, data collection and analysis, decision to publish, or manuscript preparation.

## Data Access Statement

The data presented in this study are available on request from the corresponding author.

## Ethical Compliance

All procedures performed in this study involving human participants were in accordance with the ethical standards of the institutional and/or national research committee and with 1964 Helsinki Declaration and its later amendments or comparable ethical standards.

## Author Contributions

Conceptualization: J.S. and M.B.; methodology: J.S. and M.B.; validation: J.S. M.B. and J.Ś.; formal analysis: J.S; investigation: J.S and J.Ś.; resources: J.S., M.B. and J.Ś.; data curation: J.S.; writing— original draft preparation: J.S.; writing—review and editing: J.S., M.B. and J.Ś.; visualization: J.S.; supervision: M.B.; project administration: M.B. All authors have read and agreed to the published version of the manuscript.

## References

1. Ngo TD, Kashani A, Imbalzano G, Nguyen KTQ, Hui D. Additive manufacturing (3D printing): A review of materials, methods, applications and challenges. Compos Part B Eng. 2018 Jun;143:172–96.
2. Additive Manufacturing by Technology by Printer Type by Material by Application by Component and by End-User - Global Opportunity Analysis And Industry Forecast 2022-2030 [Internet]. Research and Markets. [cited 2023 May 21]. Available from: https://www.researchandmarkets.com/reports/5699786/additive-manufacturing-by-technology-by-printer
3. ISO/ASTM 52900:2021 - Additive manufacturing — General principles — Fundamentals and vocabulary [Internet]. ISO. [cited 2023 May 21]. Available from: https://www.iso.org/standard/74514.html
4. Li L, Liu W, Sun L. Mechanical characterization of 3D printed continuous

carbon fiber reinforced thermoplastic composites. Compos Sci Technol. 2022 Aug; 227:109618.
5. Elkaseer A, Chen KJ, Janhsen JC, Refle O, Hagenmeyer V, Scholz SG. Material jetting for advanced applications: A state-of-the-art review, gaps and future directions. Addit Manuf. 2022 Dec; 60:103270.
6. Pagac M, Hajnys J, Ma QP, Jancar L, Jansa J, Stefek P, et al. A Review of Vat Photopolymerization Technology: Materials, Applications, Challenges, and Future Trends of 3D Printing. Polymers. 2021 Feb 17; 13(4):598.
7. Mostafaei A, Elliott AM, Barnes JE, Li F, Tan W, Cramer CL, et al. Binder jet 3D printing—Process parameters, materials, properties, modeling, and challenges. Prog Mater Sci. 2021 Jun; 119:100707.
8. Zhuo P, Li S, Ashcroft IA, Jones IA. Continuous fibre composite 3D printing with pultruded carbon/PA6 commingled fibres: Processing and mechanical properties. Compos Sci Technol. 2022 Apr;221:109341.
9. He Q, Wang H, Fu K, Ye L. 3D printed continuous CF/PA6 composites: Effect of microscopic voids on mechanical performance. Compos Sci Technol. 2020 May;191:108077.
10. Chou TW. Two-dimensional textile structural composites. In: Microstructural Design of Fiber Composites [Internet]. Cambridge: Cambridge University Press; 1992. p. 285–373. (Cambridge Solid State Science Series). Available from: https://www.cambridge.org/core/books/microstructural-design-of-fiber-composites/twodimensional-textile-structural-composites/258021BCE42DFD5B004B81B2CD471451
11. Poniecka A, Barburski M, Ranz D, Cuartero J, Miralbes R. Comparison of Mechanical Properties of Composites Reinforced with Technical Embroidery, UD and Woven Fabric Made of Flax Fibers. Materials. 2022 Oct 25;15(21):7469.
12. O'Connor HJ, Dickson AN, Dowling DP. Evaluation of the mechanical performance of polymer parts fabricated using a production scale multi jet fusion printing process. Addit Manuf. 2018 Aug;22:381–7.
13. ISO 14125:1998 - Fibre-reinforced plastic composites — Determination of flexural properties.
14. ISO 527-4:2021 - Plastics - Determination of tensile properties - Part 4: Test conditions for isotropic and orthotropic fibre-reinforced plastic composites.
15. ISO 527-1:2019 - Plastics - Determination of tensile properties - Part 1: General principles.
16. Barburski M, Masajtis J. Modelling of the change of structure of woven fabric under mechanical loading. Fibres Text East Eur. 2009 Jan;No 1(72).
17. Gliszczynski A, Kubiak T. Progressive failure analysis of thin-walled composite columns subjected to uniaxial compression. Compos Struct. 2017 Jun;169:52–61.
18. Liu D, Tang M, Yan J. Comparative study of the tensile properties of 2D and UD over-braided multilayer composites. Compos Sci Technol. 2021 Jul;210:108817.
19. Vanleeuw B, Carvelli V, Lomov S, Barburski M, Vuure AW. Deformability of a Flax Reinforcement for Composite Materials. Key Eng Mater. 2014 May;611–612:257–64.
20. Bullock RE. Strength Ratios of Composite Materials in Flexure and in Tension. J Compos Mater. 1974 Apr;8(2):200–6.
21. Vanleeuw B, Carvelli V, Barburski M, Lomov SV, Van Vuure AW. Quasi-unidirectional flax composite reinforcement: Deformability and complex shape forming. Compos Sci Technol. 2015 Apr;110:76–86.
22. Lemmi TSh, Barburski M, Samuel BT. Analysis of Mechanical Properties of Unidirectional Flax Roving and Sateen Weave Woven Fabric-Reinforced Composites. Autex Res J. 2021 Jun 1;21(2):218–23.